

## Original Article

# Cone-Beam CT Compared to Multi-Slice CT for the Diagnostic Analysis of Conductive Hearing Loss: A Feasibility Study

Pieter Kemp , Jiska Van Stralen , Pim De Graaf , Erwin Berkhout , Pepijn Van Horsen , Paul Merkus 

Department of Otolaryngology-Head and Neck Surgery, Ear & Hearing, Amsterdam University Medical Centers, Vrije Universiteit Amsterdam, Amsterdam Public Health Research Institute, Amsterdam, The Netherlands (PK, JS, PM)

Department of Radiology and Nuclear Medicine, Amsterdam University Medical Center – Location VUmc, Amsterdam, The Netherlands (PDG)

Department of Oral and Maxillofacial Radiology Academic Center for Dentistry Amsterdam, Amsterdam, The Netherlands (EB)

Department of Physics and Medical Technology, Amsterdam University Medical Center – Location VUmc, Amsterdam, The Netherlands (PVH)

ORCID iDs of the authors: P.K. 0000-0001-8453-9473; J.V.S. 0000-0001-6575-3001; P.D.G. 0000-0003-1938-0747; E.B. 0000-0002-0718-6763; P.V.H. 0000-0002-0917-0060; P.M. 0000-0002-5859-7386.

Cite this article as: Kemp P, Van Stralen J, De Graaf P, Berkhout E, Van Horsen P, Merkus P. Cone-Beam CT Compared to Multi-Slice CT for the Diagnostic Analysis of Conductive Hearing Loss: A Feasibility Study. J Int Adv Otol 2020; 16(2): 222-6.

**OBJECTIVES:** Multislice computed tomography (MSCT) is commonly used as a diagnostic tool for patients with a conductive hearing loss. Recent studies indicate that cone-beam computed tomography (CBCT) may be used as a low-radiation dose alternative for temporal bone imaging. This study compares image quality and radiation dose between CBCT and MSCT when assessing anatomical landmarks related to conductive hearing loss.

**MATERIALS and METHODS:** Five human cadaver heads (10 ears) were imaged on the NewTom 5G CBCT and the Discovery CT750 HD MSCT. Visibility of 16 anatomical landmarks of the middle and inner ear was assessed by two observers on a 4-point Likert scale. Furthermore, effective radiation dose was compared, and contrast-to-noise ratio and spatial resolution were measured with a phantom head.

**RESULTS:** Image quality of CBCT was assessed as superior to MSCT. Effective radiation dose of the high-resolution CBCT protocol was 30.5% of the clinical MSCT dose. High-resolution CBCT was reported as having a higher spatial resolution and superior contrast-to-noise perception in comparison with MSCT.

**CONCLUSION:** High-resolution CBCT was evaluated as superior to MSCT in the assessment of structures related to conductive hearing loss. Furthermore, CBCT imaging resulted in a considerably lower effective radiation dose.

**KEYWORDS:** Cone-beam computed tomography, multislice computed tomography, temporal bone imaging, conductive hearing loss, radiation dosage

## INTRODUCTION

In current practice, multislice computed tomography (MSCT) is typically the standard imaging method used to assess a patient with conductive hearing loss. However, not all clinically important structures are very well visible with MSCT. In particular, pathology of the ossicular chain can be hard to identify. Clinically, this shortcoming of MSCT leads to patients with conductive hearing loss in which existing pathology cannot be accurately visualized. Recent research indicates that cone-beam computed tomography (CBCT) may prove to be an alternative <sup>[1]</sup>.

Cone-beam computed tomography is commonly used as a diagnostic tool for imaging the dental and the maxillofacial region. CBCT is a modified computed tomography (CT) technique based on the rotation of a cone-shaped x-ray beam around the patient. The technique was first introduced in the late 1990s; since then, the diagnostic power of CBCT has improved rapidly <sup>[2]</sup>. CBCT has some specific advantages over MSCT. In general, CBCT has a significantly lower radiation dose, higher spatial resolution, and pro-

A pilot for this study was presented at the CHOLE 2016 Conference, June 5-8, 2016, Edinburgh, Scotland.

**Corresponding Address:** Paul Merkus E-mail: P.Merkus@vumc.nl

**Submitted:** 08.04.2018 • **Revision Received:** 02.16.2019 • **Accepted:** 03.26.2019

Available online at [www.advancedotology.org](http://www.advancedotology.org)



Content of this journal is licensed under a  
Creative Commons Attribution-NonCommercial  
4.0 International License.

duces fewer metal artifacts [3-7]. On the basis of these advantages and available research, CBCT may be an interesting alternative to MSCT.

The potential of CBCT is increasingly being investigated in non-dental regions, including various ear, nose, and throat (ENT) regions such as the temporal bone, skull base, and sinus [4].

Studies on temporal bones concluded that CBCT is at least as accurate as MSCT when assessing the visibility of clinically important anatomic structures [1, 8-10]. CBCT has also been described as suitable and, in many ways, equivalent to MSCT for postoperative cochlear implant (CI) imaging [5, 11, 12] and in the assessment of otosclerosis [13]. Furthermore, a prototype mobile C-arm for intraoperative CBCT has been developed, which showed little difference in image quality when compared with MSCT [14].

However, few comparative clinical studies have been conducted [5, 13, 15, 16] and little research has specifically focused on the potential role of CBCT in assessing anatomic structures related to the ossicular chain or causes of conductive hearing loss.

This study was set out to compare image quality and radiation dose between high-resolution CBCT and MSCT. Clinically available CBCT scanners showed considerable differences in image quality, the scanner with the most potential was selected for this study. Image quality was assessed as the visibility of clinically important structures for conductive hearing loss. Furthermore, effective radiation dose was compared, and contrast-to-noise ratio (CNR) and spatial resolution were measured with a phantom head.

## MATERIALS AND METHODS

### Data Acquisition

Five formalin-fixed human cadaver heads (10 ears) from the Department of Anatomy and Neurosciences were prepared for imaging by paracentesis. Images were collected with the NewTom 5G (QR, Verona, Italy) CBCT and the Discovery CT750 HD (GE Healthcare, Milwaukee, Wisconsin, USA) MSCT. Scan settings and protocols were optimized by radiologists with expertise in CBCT and MSCT. NewTom 5G scan parameters were voltage, 110 kV; current, 20 mA; exposure time, 7.3 seconds; field of view (FOV), 8 × 8 cm; pixel spacing, 0.15 × 0.15 mm; and slice thickness 0.25 mm; and a high-resolution filter was used. Discovery CT750 HD scan parameters were voltage, 120

kV; current, 400 mA; exposure time, 0.7 seconds; FOV, 15 × 5 cm; pixel spacing, 0.3 × 0.3 mm; and slice thickness 0.625 mm; and detail-enhancing kernel (Boneplus) was used for image reconstruction. Furthermore, spatial resolution and CNR were evaluated by scanning the Catphan 500 phantom (The Phantom Laboratory, Salem, Massachusetts, USA).

### Image Analysis

For image quality evaluation, each image was independently analyzed by an ear, nose throat (ENT) surgeon and a neuroradiologist, with 13 and 7 years of experience in ear imaging, respectively. To achieve a quantitative assessment for image quality, visibility of 16 anatomical landmarks related to conductive hearing loss (shown in Table 1) was evaluated by using a 4-point Likert scale (1=*not visible*, 2=*poorly visible*, 3=*adequately visible*, 4=*very well visible*). Blinding was not applicable because CBCT and MSCT images were differentiable. Still, the scans were randomly assessed.

### Phantom Image Analysis

Spatial resolution was assessed from scans of the CTP528 phantom module in the Catphan 500 phantom. The module consists of 21 sets of line pairs with progressively smaller gap sizes ranging from 0.5 cm to 0.024 cm. The smallest differentiable line pair was identified by visual evaluation of the images by an experienced medical physicist and radiologist.

Contrast to-noise-ratio (CNR) was determined as a quantitative measurement of image quality. The CNR was defined as the mean pixel intensity difference in the outer auditory canal air volume and the bone region around the cochlea, divided by the standard deviation of the pixel intensity in a uniform section of phantom scans at the level of the bone region, similar to Peltonen et al [1]. Circular regions of interest were drawn by a medical physicist (verified by the first author) and used to obtain the mean and standard deviation intensity values. Image analysis was performed with ImageJ (version 1.51h; National Institutes of Health, Bethesda, Maryland, USA).

### Statistical Analysis

To test for differences between scanners, total scores of all landmarks and scores of subgroups (such as the ossicular chain) were compared between the scanners. For the total score and the scores of the subgroups, linear mixed models with fixed effect for type of scanner

## MAIN POINTS

- Image quality of anatomical landmarks was compared between high-resolution cone-beam CT (CBCT) and multislice CT (MSCT). Furthermore, radiation dose, contrast-to-noise ratio and spatial resolution were compared.
- Image quality of CBCT was assessed as superior to MSCT with a higher spatial resolution and superior contrast-noise perception.
- Effective radiation dose of the high-resolution CBCT protocol was 30% of the clinical MSCT dose.
- CBCT imaging of the middle ear has been shown to be a feasible imaging method, with high clinical potential.

**Table 1.** List of anatomical landmarks

Ossicular chain	Other middle ear and inner ear structures
1. Incudomalleolar joint	8. Round window
2. Anterior malleolar ligament	9. Facial canal (tympanic portion)
3. Long process of incus	10. Cochleariform process
4. Incudostapedial joint	11. Tegmen tympani
5. Head of stapes	12. Chorda tympani
6. Crura of stapes	13. Tympanic membrane
7. Footplate	14. Cochlear aqueduct
	15. Vestibular aqueduct
	16. Modiolus

and random effect for temporal bone were used. All statistical analysis was performed using Statistical Package for the Social Sciences (SPSS) for Windows, version 25.0 (IBM Corp., Armonk, NY, USA). Kappa values were not reliable because of the small sample size.

Cone beam computed tomography and MSCT both reported a dose-length product (DLP) after scanning. The DLP was multiplied by a conversion factor to calculate an effective dose [17]. This conversion factor of 0.0019 mSv-mGy<sup>-1</sup> is applicable to a CT of the head and based on the International Commission on Radiological Protection 103 [18].

**RESULTS**

**Image Quality**

Image quality of the selected CBCT was assessed as superior to MSCT (p<0.001), as shown in Table 2. Similar significant differences were found when comparing the subgroups, the ossicular chain (p<0.001) and the middle and inner ear (p=0.001). When comparing visibility of individual landmarks (see Table 1 of the online supplement for an overview), footplate, facial canal (tympanic portion), cochlear aqueduct, and vestibular aqueduct were significantly better visible with CBCT compared with MSCT (p<0.05). Examples of corresponding images of MSCT and CBCT can be seen in Figure 1.

**Table 2.** Overview of mean total and mean subgroup scores

Computed tomography device	Multislice computed tomography	Cone-beam computed tomography
Ossicular chain	2.42 (0.93)	2.76** (0.92)
Middle and inner ear	2.16 (0.97)	2.49** (1.02)
Total	2.27 (0.96)	2.61** (0.99)

\*\*p<0.01.

Mean scores and standard deviations of the computed tomography devices. All landmarks have 20 scores (10 ears x 2 observers) based on a 4-point Likert scale. Mean scores were derived from all scores in the (sub)group.

The long processus of the incus and the tegmen tymani were adequately visible with both systems. The chorda tympani was assessed as not visible on all scans for both CBCT as MSCT.

**Dosimetry**

The DLP value of the CBCT scans was constant at 134.1 mGy-cm, compared with a mean DLP of 432.0 mGy-cm (range: 377.29-462.44) for MSCT. By multiplying with the conversion factor, the effective dose of CBCT was 69.5% less compared with MSCT (0.25 mSv and 0.82 mSv, respectively).

**Phantom Analysis**

For MSCT, the smallest differentiable gap size (spatial resolution) corresponded to 0.036 cm. For CBCT even the smallest gap size (line pair 21) was still differentiable; therefore, the spatial resolution of the system was at least 0.024 cm. Both results are in accordance with the pixel spacing of the scan parameters.

The average CNR value of the MSCT and CBCT images was 27.2 [standard deviation (SD): 3.4] and 48.6 (6.7 SD), respectively. The difference in CNR value was found to be significant (p<0.001) using a nonpaired two-tailed t-test.

**DISCUSSION**

Image quality of CBCT was assessed as superior to MSCT. Furthermore, effective radiation dose of high-resolution CBCT was 69.5% less, compared with the effective radiation dose of MSCT. Results indicate that CBCT is a promising CT technique for scanning the temporal bone of patients with conductive hearing loss, but it is dependent on the type of scanner and scan settings.

Previous studies showed that CBCT can provide comparable image quality to MSCT.

Temporal bone studies [1, 8, 10, 14] concluded that CBCT is comparable to MSCT when assessing visibility of clinically important anatomic struc-

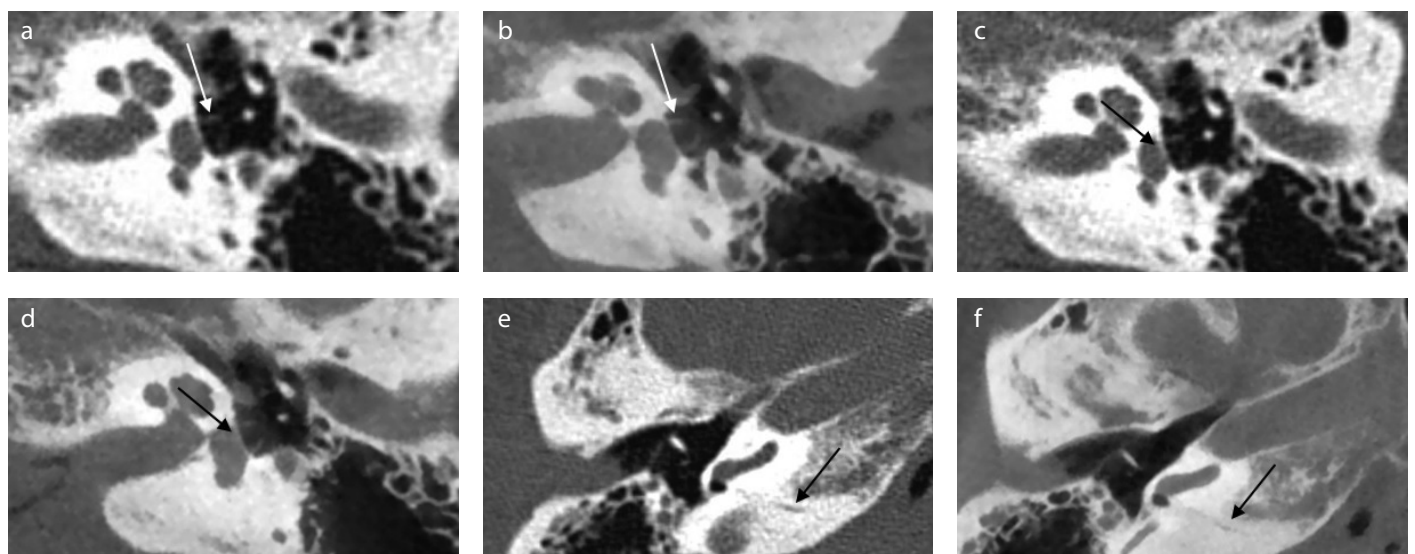


**Figure 1.** a-f. Example of corresponding images of multislice computed tomography (MSCT) and cone-beam computed tomography (CBCT). Images of MSCT (a, c, e) and corresponding images of CBCT (b, d, f). In these images stapes crurae, footplate, and cochlear aqueduct are clearly visible on CBCT. (a, b) Crurae of stapes (axial view). (c, d) Footplate (axial view) (e, f) Cochlear aqueduct (axial view). Cadaver heads were scanned in slightly different angles, because of which, the corresponding images might be in slightly different planes. During the assessment, images were turned and tilted for optimal comparison.

tures. Postoperative CI imaging studies <sup>[5, 11, 12]</sup> showed no significant differences in the overall image quality between CBCT and MSCT as well. In previous cadaver studies temporal bones <sup>[1, 9, 10]</sup>, the temporal bones placed within a custom head phantom <sup>[14]</sup> or hemi-cadaver heads <sup>[8]</sup> were used, which may have affected the results.

In contrast to earlier studies, the results of this study indicate that the image quality of high-resolution CBCT could be superior to MSCT. This can be explained by the ongoing introduction of more powerful CBCT systems that have the capacity to perform high-resolution temporal bone scans <sup>[4]</sup>. For instance, CBCT scan settings were set on high resolution, in which scans were assessed with a slice thickness of 0.15 mm, whereas most CBCT scans in the previous studies were assessed with considerably thicker slices <sup>[11, 13-15]</sup>.

Some CBCT scanners used in the previous studies are specifically designed for dental and maxillofacial imaging. These scanners cannot deliver the power needed to visualize anatomical landmarks of the temporal bone properly, which are extremely small in size and are located in or around dense bone <sup>[4]</sup>.

The contrast perception of CBCT is generally considered inferior to the MSCT imaging, especially with regard to low-contrast differences in soft tissues <sup>[3]</sup>. Our phantom analysis of the CNR however shows a two-fold increase in CNR in favor of the CBCT. This is a direct result of a higher noise level in the MSCT images compared with CBCT, due to the detail-enhancing kernel (Boneplus) used for image reconstruction.

The Boneplus kernel is essential for the MSCT imaging of the temporal bone because it is optimized for detail enhancement of smaller structures although at the cost of noise increase.

This study had some limitations. In a clinical setting, both temporal bones of a patient need to be scanned to be able to compare deviations. A scan width of 15 cm is required to scan both temporal bones and is therefore the standard and preferred setting in temporal bone imaging. The FOV of the CBCT scans was set to 8 × 8 cm. However, image quality and radiation dose of both scan protocols (8 × 8 cm and 15 × 5 cm) are similar for the NewTom 5G CBCT <sup>[4]</sup>. Some middle ears were still filled with fluid despite paracentesis of the eardrum of all formalin-fixed human cadaver heads, which made assessing visibility of some clinically important structures more difficult. Another factor is that normal temporal bones were assessed in this study, although it has been specifically reported that CBCT can be limited in the assessment of pathology of the middle ear <sup>[16]</sup>.

Despite promising results <sup>[16]</sup> and expert remarks <sup>[4]</sup> about the potential of CBCT as an alternative diagnostic tool for patients with conductive hearing loss, additional research will be needed for more conclusive results.

An important issue for future research is that high-resolution CBCT scanning can only be achieved with a long acquisition time compared with MSCT. This makes the technique more vulnerable for motion artifacts. Especially in pediatric patients this could be of great importance. In the NewTom 5G, patients are scanned in a supine position, which may lead to a reduction of motion artifacts in patients who are unable to remain stationary in an upright position. Clinical

studies should further investigate the role of motion artifacts in high-resolution CBCT temporal bone imaging.

## CONCLUSION

This study shows the potential of high-resolution CBCT imaging of the middle ear, assessed as having better image quality and a lower radiation dose than MSCT. Clinical studies should be conducted for more conclusive results on the potential of CBCT as a diagnostic tool for patients with conductive hearing loss.

**Ethics Committee Approval:** N/A.

**Informed Consent:** N/A.

**Peer-review:** Externally peer-reviewed.

**Author Contributions:** Concept - P.K., J.V.S., P.M.; Design - P.K., J.V.S., P.M.; Supervision E.B., P.D.G., P.M.; Resource - E.B., P.V.H., P.D.G.; Materials P.K., J.V.S., P.V.H.; Data Collection and/or Processing - P.K., P.D.G., E.B., P.V.H., P.M.; Analysis and/or Interpretation - P.K., P.M.; Literature Search P.K.; Writing - P.K.; Critical Reviews - J.V.S., P.D.G., E.B., P.V.H., P.M.

**Acknowledgements:** The authors would like to thank Birgit Witte for support in the statistical analysis.

**Conflict of Interest:** The authors have no conflict of interest to declare.

**Financial Disclosure:** The authors declared that this study has received no financial support.

## REFERENCES

1. Peltonen LI, Aarnisalo AA, Kortensniemi MK, Suomalainen A, Jero J, Robinson S. Limited cone-beam computed tomography imaging of the middle ear: a comparison with multislice helical computed tomography. *Acta Radiol* 2007; 48: 207-12. [\[Crossref\]](#)
2. De Vos W, Casselman J, Swennen GR. Cone-beam computerized tomography (CBCT) imaging of the oral and maxillofacial region: a systematic review of the literature. *Int J Oral Maxillofac Surg* 2009; 38: 609-25. [\[Crossref\]](#)
3. Hodez C, Griffaton-Taillandier C, Bensimon I. Cone-beam imaging: applications in ENT. *Eur Ann Otorhinolaryngol Head Neck Dis* 2011; 128: 65-78. [\[Crossref\]](#)
4. Casselman JW, Gieraerts K, Volders D, Delanote J, Mermuys K, De Foer B, et al. Cone beam CT: non-dental applications. *JBR-BTR* 2013; 96: 333-53. [\[Crossref\]](#)
5. Razafindranaly V, Truy E, Pialat JB, Martinon A, Bourhis M, Boublay N, et al. Cone Beam CT Versus Multislice CT: Radiologic Diagnostic Agreement in the Postoperative Assessment of Cochlear Implantation. *Otol Neurotol* 2016; 37: 1246-54. [\[Crossref\]](#)
6. Offergeld C, Kromeier J, Aschendorff A, Maier W, Klenzner T, Beleites T, et al. Rotational tomography of the normal and reconstructed middle ear in temporal bones: an experimental study. *Eur Arch Otorhinolaryngol* 2007; 264: 345-51. [\[Crossref\]](#)
7. Offergeld C, Kromeier J, Merchant SN, Lasurashvili N, Neudert M, Bornitz M, et al. Experimental investigation of rotational tomography in reconstructed middle ears with clinical implications. *Hear Res* 2010; 263: 191-7. [\[Crossref\]](#)
8. Dahmani-Cause M, Marx M, Deguine O, Fraysse B, Lepage B, Escude B. Morphologic examination of the temporal bone by cone beam computed tomography: comparison with multislice helical computed tomography. *Eur Ann Otorhinolaryngol Head Neck Dis* 2011; 128: 230-5. [\[Crossref\]](#)
9. Zou J, Lahelma J, Arnisalo A, Pyykko I. Clinically relevant human temporal bone measurements using novel high-resolution cone-beam CT. *J Otol* 2017; 12: 9-17. [\[Crossref\]](#)

10. Teymoortash A, Hamzei S, Murthum T, Eivazi B, Kureck I, Werner JA. Temporal bone imaging using digital volume tomography and computed tomography: a comparative cadaveric radiological study. *Surg Radiol Anat* 2011; 33: 123-8. [\[Crossref\]](#)
11. Ruivo J, Mermuys K, Bacher K, Kuhweide R, Offeciers E, Casselman JW. Cone beam computed tomography, a low-dose imaging technique in the postoperative assessment of cochlear implantation. *Otol Neurotol* 2009; 30: 299-303. [\[Crossref\]](#)
12. Theunisse HJ, Joemai RM, Maal TJ, Geleijns J, Mylanus EA, Verbist BM. Cone-beam CT versus multi-slice CT systems for postoperative imaging of cochlear implantation—a phantom study on image quality and radiation exposure using human temporal bones. *Otol Neurotol* 2015; 36: 592-9. [\[Crossref\]](#)
13. Redfors YD, Grondahl HG, Hellgren J, Lindfors N, Nilsson I, Moller C. Otosclerosis: anatomy and pathology in the temporal bone assessed by multi-slice and cone-beam CT. *Otol Neurotol* 2012; 33: 922-7. [\[Crossref\]](#)
14. Erovic BM, Chan HH, Daly MJ, Pothier DD, Yu E, Coulson C, et al. Intraoperative cone-beam computed tomography and multi-slice computed tomography in temporal bone imaging for surgical treatment. *Otolaryngol Head Neck Surg* 2014; 150: 107-14. [\[Crossref\]](#)
15. Revesz P, Liktor B, Liktor B, Sziklai I, Gerlinger I, Karosi T. Comparative analysis of preoperative diagnostic values of HRCT and CBCT in patients with histologically diagnosed otosclerotic stapes footplates. *Eur Arch Otorhinolaryngol* 2016; 273: 63-72. [\[Crossref\]](#)
16. Pein MK, Brandt S, Plontke SK, Kosling S. Visualization of subtle temporal bone structures. Comparison of cone beam CT and MDCT. *Radiologe* 2014; 54: 271-8. [\[Crossref\]](#)
17. Deak PD, Smal Y, Kalender WA. Multisection CT protocols: sex- and age-specific conversion factors used to determine effective dose from dose-length product. *Radiology* 2010; 257: 158-66. [\[Crossref\]](#)
18. The 2007 Recommendations of the International Commission on Radiological Protection. ICRP publication 103. *Ann ICRP* 2007; 37: 1-332. [\[Crossref\]](#)
19. Güldner C, Diogo I, Bernd E, Dräger S, Mandapathil M, Teymoortash A, Wilhelm, T. Visualization of anatomy in normal and pathologic middle ears by cone beam CT. *Eur Arch Otorhinolaryngol* 2017; 274: 737-42. [\[Crossref\]](#)

**Supplemental Table 1.** Mean and standard deviation of individual anatomical landmarks for the preclinical study. All landmarks have 20 scores (10 ears × 2 observers) based on a 4-point Likert scale

Anatomical landmarks	Cone-beam computed tomography (CBCT)	Multislice computed tomography (MSCT)	p
<b>Ossicular chain</b>			
1. Incudomalleolar joint	2.90 (0.77)	2.55 (0.87)	0.164
2. Anterior malleolar ligament	2.35 (0.79)	2.05 (0.92)	0.297
3. Long process of incus	3.30 (0.71)	3.00 (0.89)	0.454
4. Incudostapedial joint	2.45 (0.97)	2.15 (0.85)	0.308
5. Head of stapes	2.80 (0.81)	2.70 (0.84)	0.412
6. Crura of stapes	2.50 (1.07)	2.25 (0.89)	0.583
7. Footplate	3.05 (0.87)	2.25 (0.89)	0.001
Ossicular chain mean	2.76 (0.92)	2.42 (0.93)	<0.001
<b>Other middle ear and inner ear structures</b>			
8. Round window	2.55 (1.12)	2.20 (1.25)	0.452
9. Facial canal (tympanic portion)	2.65 (0.91)	1.85 (0.79)	0.004
10. Cochleariform process	2.65 (0.79)	2.40 (0.73)	0.071
11. Tegmen tympani	3.30 (0.95)	3.05 (0.81)	0.495
12. Chorda tympani	1.00 (0.00)	1.00 (0.00)	_*
13. Tympanic membrane	1.85 (0.48)	2.00 (0.63)	0.551
14. Cochlear aqueduct	2.15 (0.73)	1.45 (0.50)	<0.001
15. Vestibular aqueduct	3.35 (0.65)	2.75 (0.89)	0.049
16. Modiolus	2.90 (0.54)	2.70 (0.46)	0.201
Middle and inner ear mean	2.49 (1.02)	2.16 (0.97)	0.001
Total mean	2.61 (0.99)	2.27 (0.96)	<0.001

\*Chorda tympani was assessed as not visible (1) on all scans by both CBCT and MSCT.